Irreversible Inhibition of Sodium Current and Batrachotoxin Binding by a Photoaffinity-derivatized Local Anesthetic

JOHN MCHUGH*‡, WAI MAN MOK*, GING KUO WANG*, and GARY STRICHARTZ*

*From the Anesthesia Research Laboratories, Brigham and Women's Hospital, Harvard Medical School, Boston, Massachusetts 02115; and ‡HST Affiliation, Health Science and Technology Program, Harvard Medical School and Massachusetts Institute of Technology, Cambridge, Massachusetts 02139

ABSTRACT We have synthesized a model local anesthetic (LA), *N*-(2-di-*N*-butyl-aminoethyl)-4-azidobenzamide (DNB-AB), containing the photoactivatable aryl azido moiety, which is known to form a covalent bond to adjacent molecules when exposed to UV light (Fleet, G. W., J. R. Knowles, and R. R. Porter. 1972. *Biochemical Journal.* 128:499–508. Ji, T. H. 1979. *Biochimica et Biophysica Acta.* 559:39–69.). We studied the effects of DNB-AB on the sodium current (I_{Na}) under whole-cell voltage clamp in clonal mammalian GH_3 cells and on ^{3}[H]-BTX-B binding to sheep brain synaptoneurosomes. In the absence of UV illumination, DNB-AB behaved similarly to known LAs, producing both reversible block of peak I_{Na} (IC_{50} = 26 μM, 20°C) and reversible inhibition of ^{3}[H]-BTX-B (50 nM in the presence of 0.12 μg/liter *Leiurus quinquestriatus* scorpion venom) binding (IC_{50} = 3.3 μM, 37°C), implying a noncovalent association between DNB-AB and its receptor(s). After exposure to UV light, both block of I_{Na} and inhibition of ^{3}[H]-BTX-B binding were only partially reversible (I_{Na} = 42% of control; ^{3}[H]-BTX-B binding = 23% of control) showing evidence of a light-dependent, covalent association between DNB-AB and its receptor(s). In the absence of drug, UV light had less effect on I_{Na} (post exposure I_{Na} = 96% of control) or on ^{3}[H]-BTX-B binding (post exposure binding = 70% of control). The irreversible block of I_{Na} was partially protected by coincubation of DNB-AB with 1 mM bupivacaine (IC_{50} = 45 μM, for I_{Na} inhibition at 20°C, Wang, G. K., and S. Y. Wang. 1992. *Journal of General Physiology.* 100:1003–1020.), (post exposure I_{Na} = 73% of control). The irreversible inhibition of ^{3}[H]-BTX-B binding also was partially protected by coincubation with bupivacaine (500 μM, 37°C) (post exposure binding = 51% of control), suggesting that the site of irreversible inhibition of both I_{Na} and ^{3}[H]-BTX-B binding is shared with the clinical LA bupivacaine.

INTRODUCTION

Local anesthetics (LAs) are low molecular weight organic bases which block action potentials in axons by inhibiting the sodium current. The potency of LAs for impulse

Address correspondence to Gary Strichartz, Anesthesia Research Laboratories, Brigham and Women's Hospital, Harvard Medical School, Boston, MA 02115.

J. GEN. PHYSIOL. © The Rockefeller University Press · 0022-1295/95/02/0267/21 $2.00
Volume 105 February 1995 267–287

inhibition correlates with their ability to inhibit Na^+ current, indicating that the Na channel is probably the site of LA action (see review, Butterworth and Strichartz, 1990). However, because the Na channel is located within the cell membrane, it is uncertain whether LA action involves binding to a specific receptor site on the channel protein or a primary effect on the lipid phase of the cell membrane that indirectly alters ionic channel properties (Hille, 1980).

The most potent LAs must be present in the solution bathing a nerve cell at a concentration of at least 1–10 μM to produce a 50% inhibition of I_{Na} (Courtney, 1980). Given that many of these lipophilic compounds partition into membranes at concentrations on the order of 1,000 × that in aqueous solutions, the intramembranous concentrations for 50% block of I_{Na} is 1 mM or greater. In addition, stereoselectivity for channel inhibition is poor, as enantiomers of LAs rarely have stereopotency ratios of >5 (Yeh, 1980; Postma and Catterall, 1984; Hill, Duff, and Sheldon, 1988; LeeSon, Wang, Concus, Crill, and Strichartz, 1991). Both observations imply a relatively poor fit between drug and "receptor" and a consequentially weak binding energy.

The interaction of LAs with excitable membranes has been studied in several ways. Inhibition of I_{Na} by LAs has been shown to depend on both the resting transmembrane potential and the rate of rapid depolarization of the membrane (Strichartz, 1973; Courtney, 1975; Hille, 1977). Since sodium channels are known to assume different states or conformations as a function of the transmembrane potential (Bezanilla and Armstrong, 1977; Aldrich, Corey, and Stevens, 1983) it is hypothesized that LA potency is a function of Na^+ channel state (Hille, 1977; Hondeghem and Katzung, 1977).

LA binding at a hyperpolarized holding potential (−100 mV) is thought to be a function of the ligand's ability to bind to the "resting" states of the channel which predominate at this potential. Brief depolarizations transiently shift channels from the resting state to states which, for the purposes of this paper, will be summarized as the open, conducting state and the nonconducting, inactivated state. LAs bind faster and to a greater extent to these states populated by depolarization than to resting states (Strichartz, 1973; Courtney, 1975; Hille, 1977; Chernoff, 1990; Starmer, Grant, and Strauss, 1984). Thus, high frequency stimulation causes a "phasic" (use-dependent) decrease in the population of drug-free Na channels and a corresponding use-dependent inhibition of the Na current.

In addition to interacting with LAs, the Na channel also binds several classes of natural toxins. Activator toxins, which include the alkaloids veratridine (VTD) and batrachotoxin (BTX), stabilize the Na channel in a conducting, "open" conformation. The synthesis and characterization of [^{3}H] batrachotoxinin A 20-α-benzoate ([^{3}H]-BTX-B) as a probe of the BTX binding site has been described previously (Brown, Tieszen, Daly, Wernick, and Albequerque, 1981). The inhibition of these activators' actions and binding by LAs is allosteric (Willow, Gonoit, Postma, and Caterall, 1981; Postma and Catterall, 1984; Sheldon, Cannon, and Duff, 1987; Rando, Wang, and Strichartz, 1985). That is, rather than competing with the activators for a spatially overlapping site, LAs appear to stabilize conformations of the channel which have much lower affinity for the activator ligands and thereby decrease activator binding.

In the experiments presented here, we describe the actions of the photoaffinity-

derivatized model LA, DNB-AB, as a reversible inhibitor when applied in the absence of UV light and, in the presence of UV irradiation, an irreversible inhibitor both of I_{Na} and of BTX binding to synaptoneurosomes.

MATERIALS AND METHODS

Chemicals

N-hydroxysuccinimidyl-4-azidobenzoate (HSAB) was obtained from Pierce Chemical Company (Rockford, IL), 2-Di-*N*-butylaminoethylamine (DNBAE) from Pfaltz and Bauer (Waterbury,

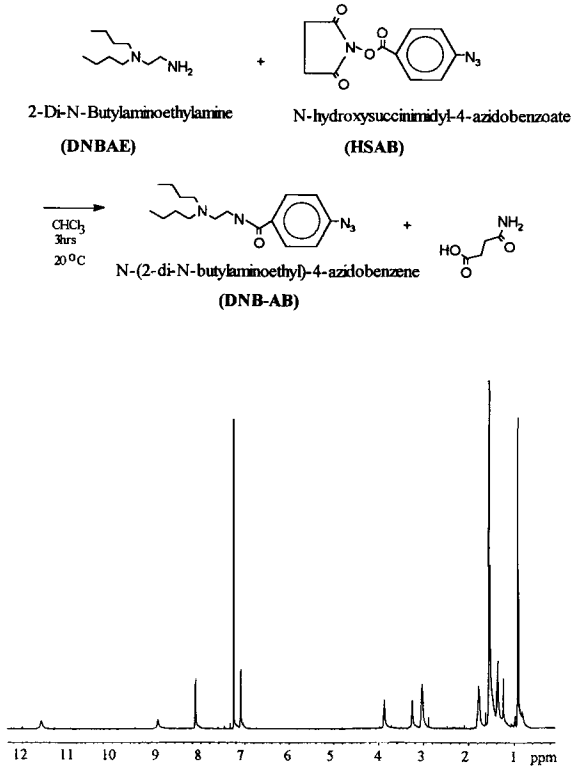

FIGURE 1. The synthesis of DNB-AB (*top*). The ^{1}H-NMR spectrum of purified DNB-AB (*bottom*). A detailed description is found at the beginning of Materials and Methods.

CT), bupivacaine and veratridine from Sigma Chemical Company (St. Louis, MO), ^{3}H-batrachotoxinin A 20-α-benzoate from DuPont-NEN (Boston, MA), and tetrodotoxin (TTX) from Calbiochem (San Diego, CA). Lyophilized scorpion venom (from *Leiurus quinquestriatus quinquestriatus*) was obtained from Latoxan, Inc. (Rosans, France).

Synthesis of DNB-AB

The synthesis of DNB-AB was accomplished in the following manner (Fig. 1). HSAB (100 mg, 0.4 mmol) was dissolved in 3 ml $CHCl_3$ and DNBAE (161 μl, 0.8 mmol) was added with continuous stirring. The reaction was allowed to proceed at room temperature (20–22°C) in darkness for 3 h. After removing the $CHCl_3$ with dry N_2, an oily yellow solid remained. The

material was purified by column chromatography (Merck Grade, 35–70 mesh) using acetonitrile:methanol (9:1, vol:vol). Purified product formed a single spot ($R_f \sim 0.64$) when eluted on thin layer chromatography plates (Fisher Brand, Redi Plate, 250 μm thickness Silica G coating with zinc silicate fluorescent indicator) in ethyl acetate:ethanol (9:1, vol:vol). The product has a pK_a of 8.6 determined potentiometrically in deionized H_2O and a molar absorptivity of 2.5×10^4 cm^{-1} M^{-1} at the absorbance maximum of 272 nm at pH = 8.0 in deionized water.

NMR

The proton NMR spectrum (500 mHz) was obtained in $CDCl_3$ (Fig. 1, *inset*) and revealed the following peaks: (δ = parts per million from TMS) δ0.93 (τ,H); 1.38 (*n*, 4H); 1.78 (*n*, 4H); 3.04 (br, s, 4H); 3.26 (br, s, 2H); 3.89 (br, s, 2H); 7.10 (d, 2H); 8.13 (d, 2H), 8.98 (br, s, 1H) which were consistent with the proposed structure of DNB-AB (Fig. 1). A peak at 7.24 was attributed to $CDCl_3$ and a peak at 1.56 was attributed to residual H_2O.

Preparation of Membrane Homogenates

Membrane homogenates were prepared as in Strichartz (1982). A New Zealand white rabbit was killed after barbiturate overdose (100 mg pentobarbital/kg) as approved by the Harvard University Standing Committee on Animals. The whole brain (8.53 gm) was removed and minced in 30 ml ice-cold homogenization solution (0.25 M sucrose, 50 mM MOPS, pH to 7.2 with NaOH) into 2 mm cubes, then homogenized in a Potter/Elvejhem (P/E) Teflon glass homogenizer (clearance ~ 0.15–0.23 mm, 10 strokes at 1,000 rpm). The homogenate was then centrifuged at 1,240 *g* in a Beckman JA-20 rotor a Beckman JL-21 ultracentrifuge for 5 min and the pellet removed and discarded. The supernatant was then spun at 40,000 *g* for 30 min. The supernatant was discarded and the pellet was resuspended in 30 ml of ice-cold Locke's solution (154 mM NaCl, 2 mM KCl, 2.2 mM $CaCl_2$, 5 mM HEPES, pH to 7.2 with NaOH). Membrane homogenates were determined to have a total protein density of 2.84 μg/μl by Peterson's modification of Lowry's protein assay (Peterson, 1977).

Photolysis Experiments

The photolysis of DNB-AB in water was effected by transillumination through the polished face of 1 × 1 × 3 cm quartz cuvettes. DNB-AB solutions (50 μM) in deionized water (pH = 8.0) were photolyzed at a distance of 10 cm with a short wave UV lamp (λ_{max} = 254 nm, 0.46 W/cm^2, model UVG-11, Ultra-Violet Products, San Gabriel, CA). Photolysis of DNB-AB in membrane homogenates was carried out by illuminating 250 μl of 1 mM DNB-AB in membrane homogenates containing 0.8 μg total protein/μl suspended in unsealed siliconized microfuge tubes (Fisher Brand, 1.5 ml). Ultraviolet light was positioned at a distance of 10 cm from the top of the suspensions. After photolysis, the suspensions were spun at 14,000 *g* for 5 min (Eppendorf 5415 tabletop centrifuge) to remove suspended membranes. The supernatant was put into quartz cuvettes, diluted to 1.5 ml with deionized water and the absorbance measured. Each sample was measured versus a reference which contained no DNB-AB but was otherwise identical. Absorbances were measured with a Gilford Response UV-Vis Spectrophotometer (Gilford Instrument Laboratories Inc., Overton, CA).

Preparation of Synaptosomes

Synaptosomes were prepared using a method adapted from Dodd, Hardy, Oakley, Edwardson, Perry, and Delaunoy (1981). A sheep (white-faced Dorset-Ewes, 40–60 kg) was killed using a barbiturate overdose according to a protocol approved by the Harvard University Standing Committee on Animals for Dr. Hal Feldman. The cerebral cortex was harvested (59 g wet

weight) and placed in 200 ml of 0.32 M sucrose at 0°C. 3–4 g sections were placed in 30 ml of 0.32 M sucrose at 0°C and were homogenized in a P/E Teflon/glass homogenizer (clearance ~0.15–0.23 mm, 12 up and down strokes at 800 rpm) while the mortar of the homogenizer was kept in an ice/water bath. The crude homogenates were pooled and distributed as 20 ml aliquots into polycarbonate centrifuge bottles. These were centrifuged at 5,100 rpm (1,500 *g*) on a 70.1 Ti rotor for 12 min at 4°C in a Beckman L-80 preparative ultracentrifuge (Palo Alto, CA). The pellet (P1) was discarded. The supernatant (nominally in 0.32 M sucrose) was removed, layered onto 8 ml of 1.2 M sucrose at 0°C and spun at 50,000 rpm (170,000 *g*) for 17 min on a 70.1 Ti rotor at 4°C. 4 ml of supernatant were removed from the gradient interface and mixed with 10 ml of 0.32 M sucrose at 0°C. The pellet (P2) and other material was discarded. The diluted interface was layered onto 8 ml of 0.8 M sucrose and spun at 50,000 rpm for 17 min on a 70.1 Ti rotor. The supernatant was discarded and the pellets (P3) were resuspended in synaptosomal storage buffer (130 mM choline·Cl, 5.5 mM glucose, 5.4 mM KCl, 0.8 mM $MgSO_4$, 50 mM HEPES, pH adjusted to 7.4 with Tris Base (~22 mM). The synaptosomes were "snap frozen" in 250 μl aliquots on ethanol/dry ice and stored at −80°C. Storage of synaptosomes in a similar fashion has been shown to have little effect on toxin binding or Na^+ flux (Tamkun and Catterall, 1981). Total protein concentration was measured to be 3.41 μg/μl after solubilizing membranes in 1.2% (wt/vol) SDS by Peterson's modification of Lowry's method (Peterson, 1977).

Whole-Cell Voltage Clamp

The whole-cell variant of the patch clamp method was used to measure Na^+ currents in GH_3 cells (see Hamill, Marty, Neher, Sackman, and Sigworth, 1981). A reverse Na^+ gradient was created across the cell membrane. This reversed gradient (see Cota and Armstrong, 1989; Wang and Wang, 1992) has the advantages that the Na^+ current is visible at all voltages and that the voltage error caused by access resistance is less serious as an ingredient in gating parameter assessment than with the inward sodium current.

GH_3 cells were maintained as described by Cota and Armstrong (1989). The petri dish that contained the GH_3 cells was first rinsed with an external solution containing (in millimolar): 150 choline-Cl, 0.2 $CdCl_2$, 2 $CaCl_2$, and 10 HEPES adjusted to pH 7.4 with TMA·OH. The dish with GH_3 cells was then used as a recording chamber (containing ~0.5 ml external solution) which was continuously perfused with the external solution at a rate of 0.5 ml/min. Washout of drug was accomplished by transiently increasing the flow to 5 ml/min until the sodium current reached a steady state (~5 min).

Micropipettes were fabricated from borosilicate capillary tubing (Drummond Scientific Co., Broomall, PA) and had tip resistances of ~1 MΩ when filled with a high Na^+ solution containing (in millimolar): 100 NaF, 30 NaCl, 10 EGTA, and 10 HEPES adjusted to pH 7.2 with CsOH.

The recording system consisted of a List EPC-7 patch clamp amplifier (List Electronic, Eberstadt, West Germany), a homemade analogue leak and capacitance subtractor and a 33 MHz 486 PC computer interfaced to the amplifier by a 100 kHz Labmaster board (Axon Instruments, Foster City, CA). Creation of voltage clamp pulses, data acquisition and data analysis were performed using pClamp software (Axon Instruments). Leak and capacitance were further subtracted by a P/4 protocol (Armstrong and Bezanilla, 1974).

The series resistance was ~3 MΩ, ~60% of which was compensated for by the amplifier. For a cell with peak current of 5 nA, the voltage drop across the uncompensated series resistance was therefore ~6 mV (Armstrong and Gilley, 1992). Membrane potentials in this paper are reported as command potentials without further correction.

Sucrose-Gap Experiments

In studies to assess the potency of DNB-AB's photolysis products we measured the concentration dependence of the reversible reduction of the compound action potential of frog sciatic nerves. For this we used the sucrose gap, as described by Hahin and Strichartz (1981), on desheathed nerve at room temperature.

BTX Binding Experiments

The technique used was adapted from McNeal, Lewandowski, Daly, and Creveling, (1985). Scorpion venom was prepared as in Wang and Strichartz (1983). Briefly, 5 mg/ml dry weight of lyophilized venom was incubated overnight in synaptosome storage buffer (see above) at 4°C and spun at 20,000 *g* for 15 min to pellet the undissolved mucopolysaccharide. The pellet was discarded and the supernatant was then used as a 5 mg nominal protein/ml solution of scorpion venom.

Incubations were carried out in a total volume of 250 μl containing synaptosomes at a final concentration of 0.8 μg total protein/μl, 50 nM ^{3}H-BTX-B (50 Ci/mmol), 1 μM tetrodotoxin, 0.03 mg *Leiurus quinquestriatus* venom, dissolved in synaptosome storage buffer (see above). Incubations for 30 min at 37°C were terminated by dilution of the reaction mixture with 3 ml of wash buffer (163 mM choline·Cl, 5 mM HEPES, 1.8 mM $CaCl_2$, and 0.8 mM $MgSO_4$ pH to 7.4 with Tris base) and filtered through Whatman GF/C filters. Filtration was accomplished by vacuum perfusion through a 10-sample filtration device (Unipore Model 25, BioRad Laboratories, Richmond, CA). Each filter was washed three times with wash buffer at 0°C (1 ml/wash, approximately several seconds per wash). Filters and filtrate were counted in 15 ml of Aquasol-2 (DuPont-NEN) on a Beckman scintillation counter (model LS6800). The counting efficiency was ~35%. Nonspecific binding was determined by parallel experiments in the presence of 300 μM veratridine. Specific binding was ~75% of total binding at 50 nM ^{3}H-BTX-B (K_d ~ 82 nM in 1 μM *Leiurus quinquestriatus* toxin; K_d of *Leiurus quinquestriatus* for enhancement at [^{3}H]-BTX-B binding = 35 nM, Catterall, Morrow, Daly, and Brown, 1981).

RESULTS

To justify the use of DNB-AB as a photoaffinity probe of the local anesthetic binding site, we first characterized its effects on the sodium current and compared the effects of DNB-AB to the effects of clinically useful local anesthetics such as lidocaine and bupivacaine.

Inhibition of I_{Na}

DNB-AB inhibits the whole-cell sodium current (I_{Na}), as measured during brief (8 ms), infrequent (0.03 Hz) depolarizations (Fig. 2). The peak current-voltage relationships for control and drug situations in one cell, shown in Fig. 2 *C*, show that 20 μM DNB-AB reduced peak I_{Na} by ~65% at positive test voltages. As shown in Fig. 2 *D*, inhibition of I_{Na} was relatively constant from 0 to +50 mV. However, inhibition became less at more negative potentials, falling to only 20% at −60 mV, a potential where currents could first be detected. In five cells the degree of inhibition at −40 mV, a voltage where control currents are substantial, ranged from 8 to 46% whereas inhibition at +40 mV ranged from 45 to 75%. The mean ratio of inhibition at −40 mV to that at +40 mV was 0.46 ± 0.11 (SEM). From these results there appears to be a voltage dependence to the inhibition of peak I_{Na} by DNB-AB in the range of potential where sodium channels are activated.

Steady state block was usually achieved within 4–5 min when applying drug via a perfusion pipette placed within 1 mm of the clamped cell. The block was reversed within several minutes when the entire dish was perfused with drug free solution at a rate of 4 ml/min (see Fig. 9 *A*). The stimulation protocol used to assay this inhibition is shown in Fig. 3 *A*. Briefly, after 30 s of holding at $E_H = -100$ mV, the cell was hyperpolarized to −130 mV for 50 ms to remove fast inactivation of drug-free channels (Cota and Armstrong, 1989). The cell was then depolarized to +30 mV for 5 ms to elicit I_{Na}.

DNB-AB caused a concentration-dependent decrease in the whole-cell peak I_{Na} measured in this way. The data are fit by a generalized Hill equation in which the $IC_{50} = 2.7 \times 10^{-5}$ M, and $n_H = 1.6$ (Fig. 3 *C*).

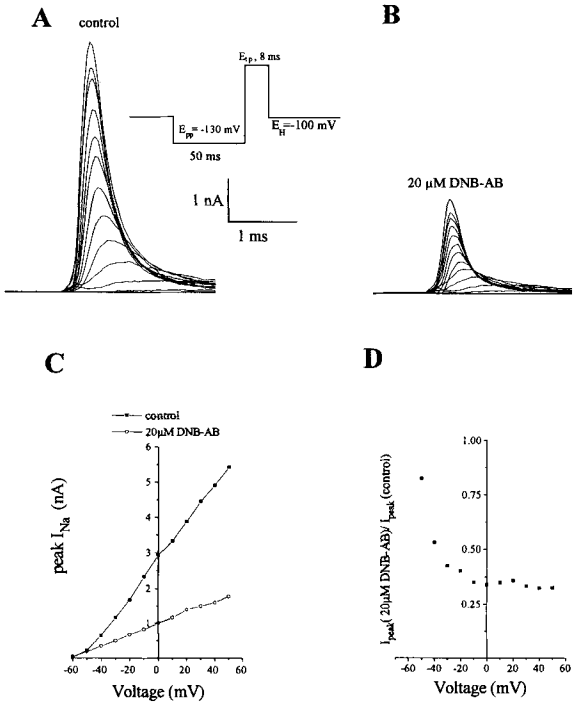

FIGURE 2. Tonic block. DNB-ABblocks I_{Na} in GH_3 cells under a reversed Na^+ gradient. (*A*) Step depolarizations from −60 to +50 mV with 10-mV increments were applied at 0.03 Hz to elicit I_{Na} in a cell bathed in drug-free solution. (*B*) 20 μM DNB-AB was applied externally and I_{Na} was measured after the drug had reached a steady state tonic block (4–5 min). (*C*) The peak current-voltage relationship both before (*filled squares*) and after (*hollow circles*) extracellular superfusion with 20 μM DNB-AB. (*D*) The ratio of peak currents ($I_{drug}/I_{control}$) is plotted versus depolarizing potential.

That $n_H > 1$ may be due to several factors. Inhibition caused by DNB-AB varies with time during each pulse. The inhibition by DNB-AB increased reversibly during the first 3 ms of the test pulse, even when the block of peak I_{Na} measured by sequential pulses (at 0.03 Hz) had reached steady state (Fig. 3 *B*). This phenomenon is reflected in changes in the time constant characterizing the decline of I_{Na} after peak current; for control cells $\tau = 0.40 \pm 0.02$ ms (SEM, $n = 3$) and for cells bathed by 20 μM DNB-AB, $\tau = 0.17 \pm 0.02$ ms ($n = 3$). The potency of DNB-AB was thus dependent on the time of measurement. Therefore, the concentration-response curve using peak I_{Na} inhibition does not yield equilibrium parameters of the drug/channel interactions, and the value of n_H obtained from a dose response curve should be interpreted with caution.

The Relationship of Channel Inactivation to Inhibition

Several mechanisms may account for the acceleration of current decay by the drug. DNB-AB may bind to open channels and block them, thereby competing with the transition of open channels to the nonconducting state(s). Alternatively, the increase in the decay rate may be the result of drug binding to an otherwise reversible, nonconducting state(s), preventing their return to an open state and reducing the prolongation of Na^+ current. Both of these mechanisms would alter the inactivating

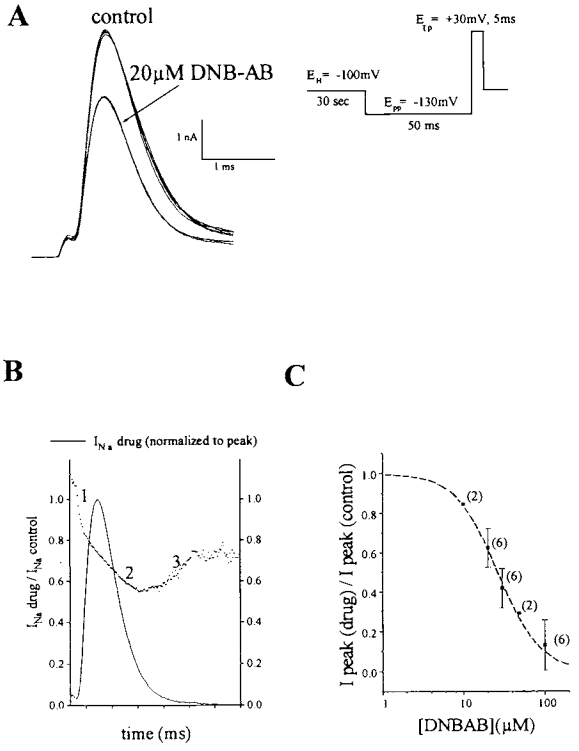

FIGURE 3. Dose response curve. (*A*) DNB-AB inhibits I_{Na} in voltage clamped GH_3 cells. (*Inset*) The pulse protocol for assessing block of I_{Na}. Once every 30 s, a hyperpolarizing prepulse to −130 mV for 50 ms was followed by a test pulse to +30 mV for 5 ms. The original current traces elicited by the protocol in both before and after exposure to 20 μM DNB-AB. In addition to decreasing the peak I_{Na}, exposure to DNB-AB also affects the time constant of current decay (control: 0.45 ± 0.01 ms (n = 3), steady state tonic block: 0.36 ± 0.01 ms [n = 3]). (Record 93824c21.) (*B*) the relative inhibition of I_{Na} increases during the depolarizing test pulse. The numbers above the dotted line refer to the development of intrapulse block of I_{Na} and are explained in the Results. A current trace in the presence of drug (*solid line*) is included for comparison. (*C*) DNB-AB caused block of I_{Na} (peak I_{Na}) at concentrations from 10 to 100 μM at low frequency (0.03 Hz). Each point represents a mean value of block and is bracketed by its standard error. The sigmoidal fit (*dashed line*) was calculated from the equation: $y = 1/(1 + ([\text{DNB-AB}]/IC_{50})n_H)$. From this fit, the IC_{50} was determined to be 27 μM with a Hill Coefficient (n_H) of 1.6.

behavior of the sodium current, as do many other local anesthetics (Courtney, 1975; Hille, 1977, 1992; Katzung and Hondeghem, 1977), so we examined this parameter and its alteration by DNB-AB.

We found that in the absence of drug, GH_3 cells show a steady time-dependent hyperpolarizing drift in the h_∞ curve. The steady state availability was measured (cf. Wang and Wang, 1992) and $h_{1/2}$ graphed as a function of the time after the whole-cell clamp was established in three cells (data not shown). These data were fit by a linear

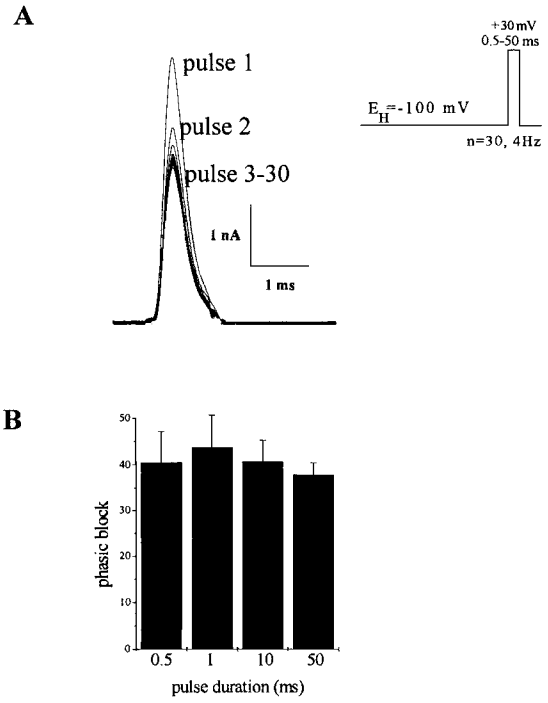

FIGURE 4. Phasic block by DNB-AB. DNB-AB produced a phasic block of I_{Na}. (*A*, *inset*) The pulse protocol used to study phasic block. 30 successive depolarizing pulses from −100 to +30 mV for 1 ms. (*A*) Current traces elicited after reaching a steady state of tonic block (4–5 min of exposure) with 20 μM DNB-AB. (*B*) The duration of the depolarizing pulse was varied from 0.5 to 50 ms, otherwise, the procedure used was the same as in *A*. Over this range of pulse duration, there was little variation in the magnitude of phasic block. Duration of depolarizing pulse also had little effect on the rate of development of phasic block. (data not shown). Depolarizing pulses of 10 ms duration were chosen for subsequent studies of phasic block.

regression analysis (cf. Hanck and Sheets, 1992), and $r^2 > 0.94$ for all fits. Means of parameters of fits were: initial $h_{1/2} = -65 \pm 5$ mV (mean ± SEM, $n = 3$) and the time-dependent drift (slope) = -0.68 ± 0.04 mV/min (mean ± SEM, $n = 3$). Therefore, over a 10-min period $h_{1/2}$ will drift by ~ -7 mV, independent of any drug related effects. Against this drug-independent drift, the effect of DNB-AB was not significant, the shifts of $h_{1/2}$ being only 5–10 mV negative (data not shown).

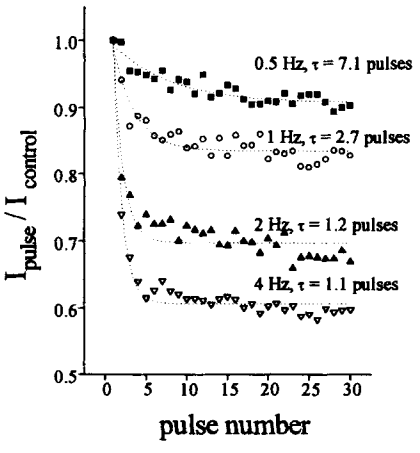

FIGURE 5. Frequency dependence of phasic block. Enhancement of block by repetitive depolarization for 10 from −100 to +30 mV in a GH_3 cell at tonic steady state block during low frequency stimulation ($f = 0.03$ Hz) (average block ~ 40%) with 20 μM DNB-AB. Accumulation of block from pulse to pulse is frequency dependent. Drug-free control traces using each pulse protocol showed <2% accumulation of block (data not shown). The data were fit with a single exponential (*dashed line*) of the form: $y = yo + Ae^{(xo-x)\tau}$ (using the software Microcal ORIGIN). The decay constant tau (τ) expressed in units of pulses for each trace is given.

Furthermore, the changes in $h_{1/2}$ that occurred during DNB-AB exposure were not reversed when the drug was removed even though inhibition of the I_{Na} was almost completely removed, reinforcing the hypothesis that the shift of $h_{1/2}$ is drug-independent while the inhibition of I_{Na} is drug dependent.

Phasic Inhibition by DNB-AB

Frequent depolarizations in the presence of DNB-AB produced additional block. Cells were held at −100 mV and depolarized to +30 mV for different durations at 4

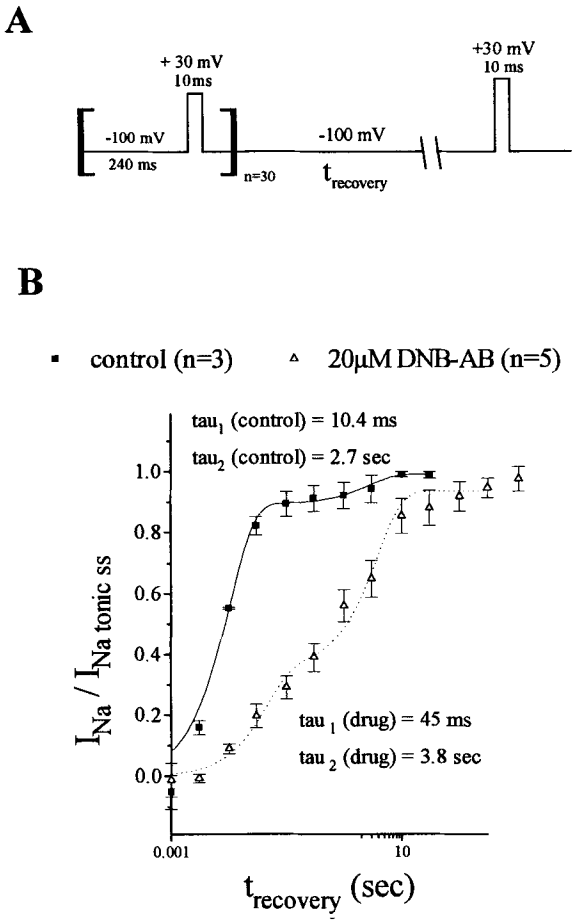

FIGURE 6. Recovery from phasic block. Recovery from phasic block of I_{Na} in the presence of 20 μM DNB-AB was assessed using the protocol shown (*A*). 30 pulses of 10 ms duration at 4 Hz were followed by a recovery period of variable duration at E_H = −100 mV and a test pulse to +30 mV to assess recovery of I_{Na}. (*B*) The amplitude of peak I_{Na} plotted versus the log of recovery time. Mean peak control currents are shown with filled squares, mean peak currents in the presence of 20 μM DNB-AB are shown with open triangles. Both are bracketed by their standard errors. The recovery time constant after 1 s was described as a single exponential with a time constant of ~3.1 s.

Hz (inset, Fig. 4 *A*). A representative set of current traces for a 1-ms depolarizing pulse is shown in Fig. 4 *A*. Varying the length of depolarization from 0.5 to 50 ms, had little effect on the amount of incremental steady state block produced by DNB-AB (Fig. 4 *B*). In addition, the rate of development of phasic block varied little with the duration of the depolarizing pulse (data not shown).

Accumulation of block from pulse to pulse in the presence of DNB-AB increased at higher frequencies of depolarization. Fig. 5 shows the relationship of peak I_{Na} to

pulse number at four different stimulation frequencies. The depolarization protocol is similar to that shown in Fig. 4 *A*, however a 10-ms depolarizing pulse was used and the frequency of stimulation was varied, as indicated in Fig. 5. As this frequency was increased, the degree of phasic block increased and the onset of phasic block quickened to a limiting value.

Recovery from Phasic Block

Phasic block of I_{Na} was fully reversible (Fig. 6). The procedure used to assay for reversibility is adapted from Castle (1991). In the presence of DNB-AB, recovery from a depolarizing pulse was slowed from control but still complete. The kinetics reveal at least two components to the recovery, one with a time constant of 45 ms, about four times that of the control current (10.4 ms), the other with a slow time constant of ~4 s, close to the slow recovery control value of ~3 s. These directly

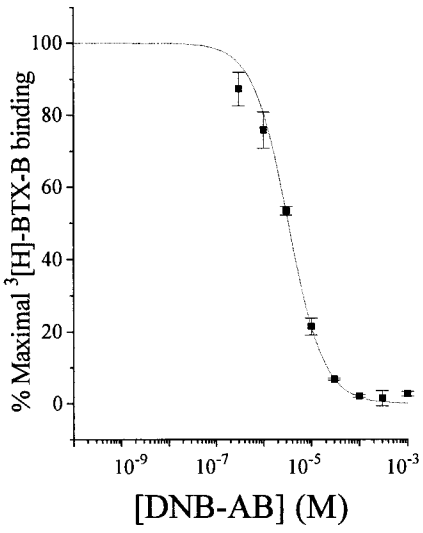

FIGURE 7. Inhibition of the specific binding of [^{3}H]-BTX-B by DNB-AB. Binding of [^{3}H]-BTX-B (50 nM) to synaptoneurosomes from sheep brain cerebral cortex at 37°C was determined in the presence of increasing concentrations of DNB-AB. Nonspecific binding of [^{3}H]-BTX-B, determined in incubations containing 300 μM VTD has been subtracted. Data points represent the means of triplicate determinations and are bracketed by standard errors. Curves were fit by the equation: $y = [100/(100 - (x/IC_{50})n_H)]$ (Microcal ORIGIN), IC_{50} = 3.3 μM n_H = 1.2.

measured recovery time constants are consistent with the frequency dependence of block enhancement shown in Fig. 5. In the control conditions, only ~10% of the current recovers slowly, but in DNB-AB this fraction is increased to ~60%, but with little change in the rate of slow recovery. It is as if the drug binds to the channels to favor the population of an endogenous, slowly recovering state. Accordingly, DNB-AB produces a reversible phasic block of I_{Na} and forms a noncovalent association with a receptor responsible for phasic block.

Inhibition of BTX Binding

The specific binding of [^{3}H]-BTX-B to synaptoneurosomes could be inhibited completely by DNB-AB in the dark. (Fig. 7). The concentration-response curve yielded an IC_{50} of 3.3 μM, and a Hill coefficient of 1.2. DNB-AB is therefore a relatively potent inhibitor of [^{3}H]-BTX binding, with an IC_{50} comparable to other

local anesthetics measured in similar assays (e.g., tetracaine IC_{50} = 3.4 μM, bupivacaine IC_{50} = 5.4 μM; McNeal et al., 1985).

Photoactivation of DNB-AB

Having established DNB-AB as a conventional LA by both electrophysiologic techniques and BTX binding studies, we explored the kinetics of the photolysis of the aryl azido moiety in an effort to develop conditions for cross-linking DNB-AB to its receptor in both GH_3 cells and sheep brain synaptosomes.

In the course of our experiments with DNB-AB, we discovered that micromolar

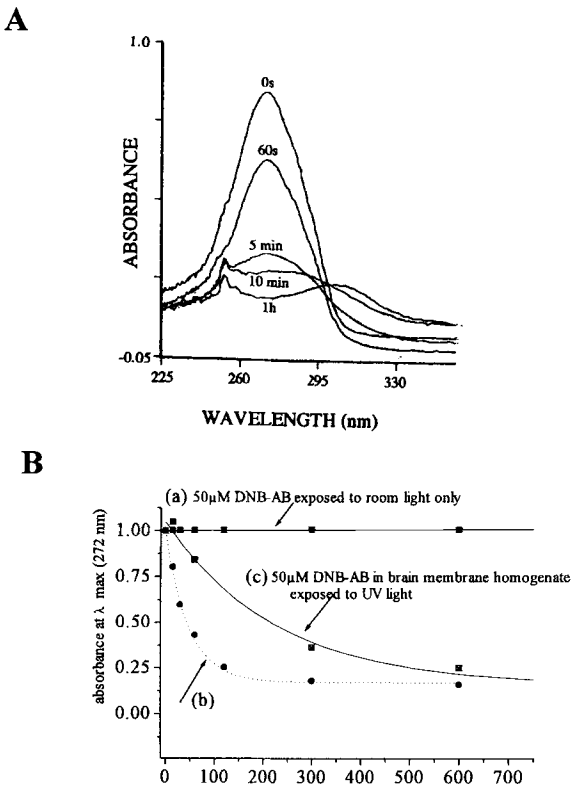

FIGURE 8. Photoactivation. (*A*) Spectral changes of DNB-AB in suspension of membranes upon exposure to UV light (18 W short wave UV lamp, λ_{max} = 254 nm, at a distance of 10 cm). Times of exposure listed near respective spectra. (*B*) Kinetics of photolysis assayed by loss of UV absorbance. A control solution kept in subdued room light showed no loss of UV absorbance over the same time period (curve *a*). The rate of photolysis was affected by the solution in which the chromophore was suspended. In curve *b*, DNB-AB was dissolved in water, and photolyzed as described above. In curve *c*, the same experiment was repeated in a suspension of membrane homogenates from rabbit brain diluted to a total protein density of 0.1 μg protein/μl of solution. The addition of membrane homogenates retarded the photolysis of DNB-AB. A control solution of DNB-AB in membrane homogenate showed little change in UV absorption when kept in subdued room light (data not shown, A_{272} ~2% over 1 h in membrane homogenate.)

solutions absorbed UV light with λ_{max} = 272 nm and $\epsilon_{272} = 2.5 \times 10^4\ M^{-1}\ cm^{-1}$ (in deionized H_2O, pH = 8.0). The absorbance at 272 nm diminished after exposure to UV light (Fig. 8). We used these data as a guide to developing experimental conditions for the cross-linking of DNB-AB to its receptor, using the likely assumption that the UV induced modification of DNB-AB responsible for the spectral

changes coincides with the modification of DNB-AB that allows cross-linking to its receptor.

DNB-AB is chemically stable when kept in aqueous solution at room temperature in subdued room light (Fig. 8, curve *A*). The conditions used were chosen to resemble those used in cross-linking DNB-AB to voltage clamped GH_3 cells (see Materials and Methods). The photoconversion of DNB-AB in deionized H_2O was rapid; the half time was ~50 s and after 200 s of exposure, the reduction in UV absorbance was essentially complete. Photoconversion of DNB-AB in suspensions of brain homogenates was slower, with half times of ~400 s, probably due to the reduced penetration of UV light in the dense synaptosomal suspension ($A_{272} = 0.72$ for a solution of homogenate similar to the one in which photolysis was performed). These conditions were chosen to mimic the UV exposure used in BTX cross-linking experiments (see Materials and Methods). We assumed that the effect on the rate of photoconversion in sheep brain synaptosomes and in rabbit brain homogenates at the same total protein concentration would be comparable.

The pharmacological activity of exhaustively photolyzed DNB-AB was assayed by comparing the inhibition of 70 μM photolysis product with that of 0–75 μM concentrations of intact DNB-AB, using the sucrose-gap method (see Materials and Methods). The activity of the product was indistinguishable from the control and clearly less than the effects from 10 μM DNB-AB. We conclude that photolysis decreases DNB-AB's potency to <0.15 of the intact molecule.

UV-dependent Irreversible Block

DNB-AB produced an irreversible block of I_{Na} when cells treated with drug were exposed to ultraviolet light. In the absence of UV light, exposure of GH_3 cells to 100 μM DNB-AB while held at −100 mV produced ~90% inhibition of the peak sodium current. This block reversed, with current recovering to 88% of control after several minutes of washing with drug-free solution. (single-cell record, Fig. 9 *A;* five-cell mean, Fig. 10).

GH_3 cells exposed to 100 μM DNB-AB while being irradiated by UV light show similar levels of block of I_{Na}. However, I_{Na} does not recover to the same extent as nonirradiated controls during drug washout. Even when washout was continued for longer periods of time, I_{Na} did not recover to the level of the drug exposed cells that had not been irradiated (42% of control current, single-cell record, Fig. 9 *B;* four-cell mean, Fig. 10). This indicates an irreversible effect of DNB-AB on some cellular component which has a direct effect on I_{Na}, but it offers no proof that this effect is at the site of the local anesthetic receptor.

We then attempted to show that the effect of DNB-AB on I_{Na} was specific to the binding site of local anesthetics. When we attempted to perform the cross-linking of local anesthetic as described above in the presence of a large excess of bupivacaine (1 mM or approximately × its IC_{50}), the irreversible inhibition of I_{Na} was significantly attenuated as I_{Na} recovered to 73% of its control value (single-cell record, Fig. 9 *C;* three-cell mean, Fig. 10).

UV light alone had little effect on the whole cell current when voltage clamped cells were exposed under conditions that produced significant irreversible block in the presence of DNB-AB (Fig. 9 *D*). We conclude that the effects of DNB-AB on I_{Na}

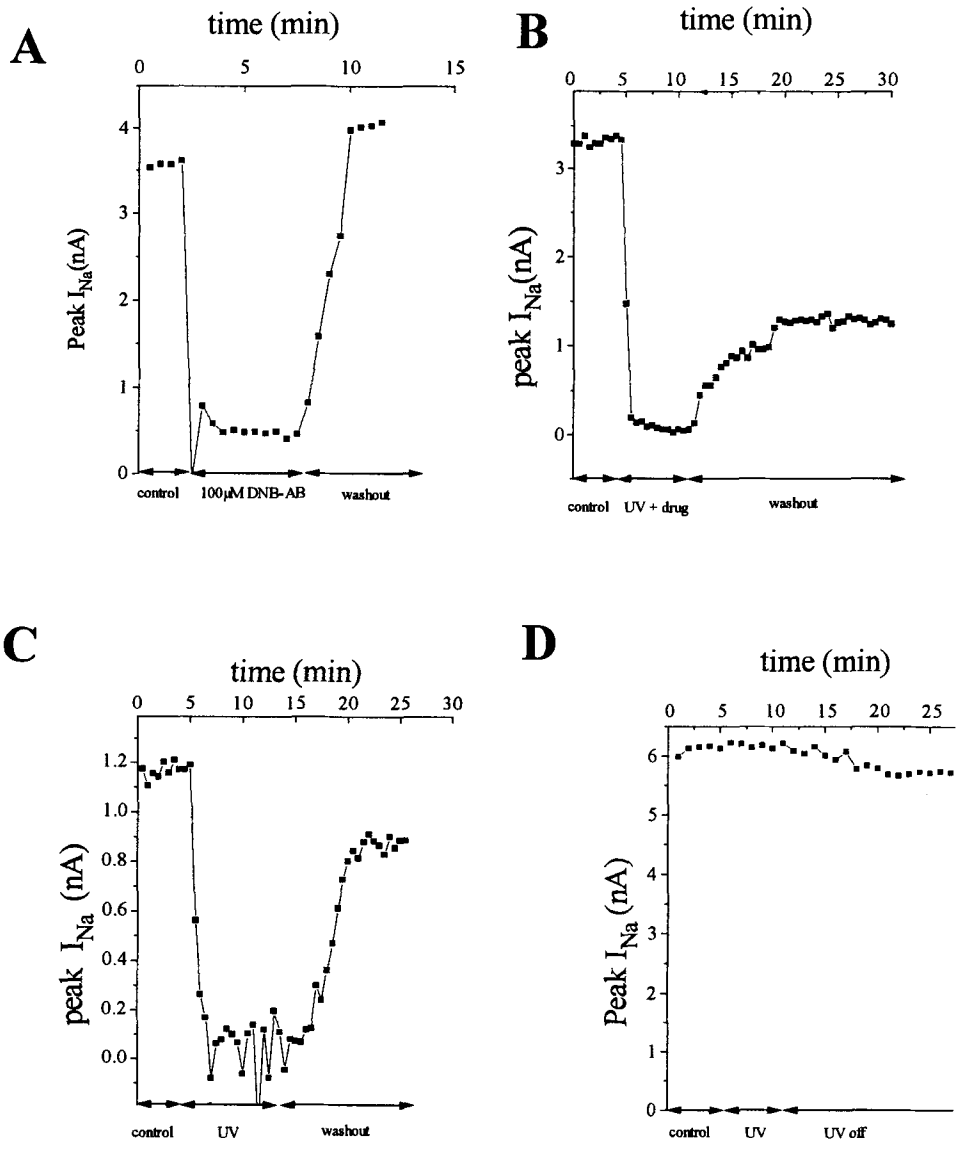

FIGURE 9. Sample current traces showing the effects of DNB-AB. Sample current traces showing peak I_{Na} versus time of a voltage clamped GH_3 cells in a reversed Na^+ gradient (0 mM outside/130 mM inside) at 21°C. Pulse protocol used to produce I_{Na} is identical to that in Fig. 3 *A*. Peak currents were measured from individual current traces using CLAMPAN software (Axon Instruments). (*A*) 100 μM DNB-AB applied in subdued room light for 5 min shows block of peak I_{Na} but no residual effect after washout. (Records 93705c01-2.) (*B*) DNB-AB applied to the cell as in *A* but in the presence of UV light (see Methods). The whole cell peak I_{Na} did not recover to its previous value even after prolonged washout (15 min shown). (Records 93514c09-11.) (*C*) When drug exposures were done in the presence of 1 mM bupivacaine (IC_{50} ~ 45 μM), the whole-cell peak I_{Na} recovers to near its preexposure value. (Record 93709c04.) (*D*) UV light has little effect on the whole cell I_{Na}. (Record 93709c12.)

under UV light are primarily the result of an irreversible interaction of the drug with the local anesthetic receptor.

Irreversible Effects of DNB-AB on [^{3}H]-BTX-B Binding

In addition to its effects on I_{Na}, DNB-AB showed high potency inhibition of [^{3}H]-BTX-B binding (IC_{50} = 3.3 μM, 37°C). When DNB-AB was applied at a concentration of ~15 μM (5 × IC_{50}), [^{3}H]-BTX-B binding was substantially inhibited (< 10% of drug-free binding, see Fig. 7). We incubated synaptosomes with 15 μM DNB-AB for 30 min at 37°C, then exposed these preincubated synaptosomes to UV light for 1 min. After washing, [^{3}H]-BTX-B binding was substantially inhibited (to 23 ± 4% of control binding, or 77 ± 4% inhibition, cf. Fig. 11). This inhibition was significantly greater than the sum of inhibition of 48 ± 9% caused by residual DNB-AB (18 ± 5%) plus that from UV light alone (30 ± 4%).

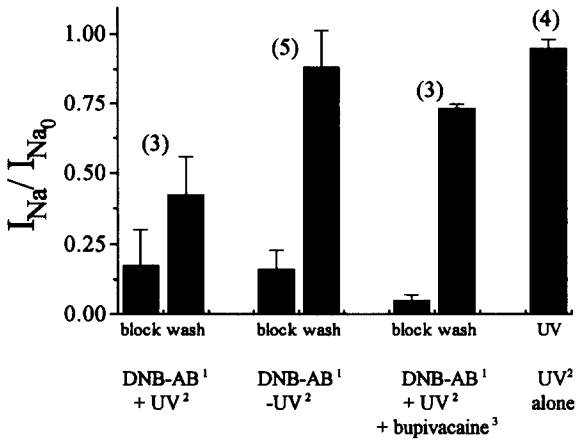

FIGURE 10. Irreversible tonic block after UV exposure. DNB-AB shows irreversible inhibition of low frequency block (f = 0.03 Hz) (Pulse protocol as in Fig. 4 *A*) of the whole-cell I_{Na}. (*1*) Drug exposures lasted for 5 min and contained 100 or 500 μM DNB-AB (IC_{50} ~25 μM). (*2*) 5-min exposure to UV light at distance = 10 cm. (*3*) 1 mM bupivacaine (K_i ~ 45 μM). Recovery from block after exposure of cells to 100 μM DNB-AB in the presence of UV light was 42 ± 13% (mean ± SEM) while block in the absence of UV light was nearly completely reversible (88 ± 3%). UV light alone induced a small decrement in the Na current (I_{Na} after exposure was 94 ± 3% of control). The irreversible effects of DNB-AB on the whole-cell I_{Na} were prevented by coincubation with 1 mM bupivacaine (I_{Na} recovered to 73 ±% of control).

Protection with Bupivacaine

Protection experiments were performed using bupivacaine at concentrations which should create high occupancy of the local anesthetic receptor site(s) (500 μM; IC_{50} = 5.4 μM, 37°C; McNeal et al., 1984). Synaptosomes were incubated with 500 μM bupivacaine for 30 min at 37°C, then exposed to UV light for 1 min, washed to remove bupivacaine and then assayed for [^{3}H]-BTX-B binding (see Materials and Methods). Binding in these experiments (70 ± 2%, mean ± SEM, n = 15, of control binding) was little different from that in synaptosomes exposed to UV light alone (70 ± 4% of control, n = 6), indicating that: (*a*) bupivacaine could be successfully

removed from the synaptosomes and (*b*) that bupivacaine did not alter the effects of UV light on subsequent BTX-B binding.

When synaptosomes were incubated with both 500 μM bupivacaine and 15 μM DNB-AB for 30 min, then irradiated, washed, and assayed for binding as described previously, binding was 51 ± 2% of control binding. Therefore, 49 ± 2% of binding was lost due to residual effects of UV and DNB-AB. This value is the same as that due to residual DNB-AB and separately applied UV light (48 ± 9%, see above) and shows that bupivacaine fully prevents the photo-induced linking of DNB-AB responsible for the irreversible inhibition of ^{3}H-BTX-B binding.

In theory, bupivacaine could prevent the photoconversion of DNB-AB by absorbing the activating UV light; then the observed "protection" by bupivacaine would not occur by membrane binding. This possibility was eliminated by the results of experiments in which the absorbance changes at 272 nm due to DNB-AB's photoconversion were shown to be identical in control solutions and those containing bupivacaine at 0.25–1.0 mM concentrations.

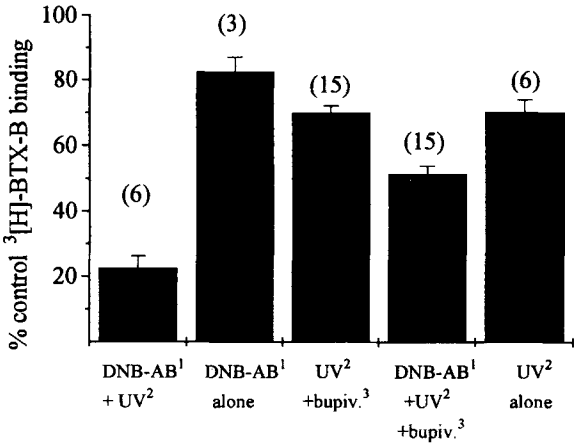

FIGURE 11. Irreversible inhibition of the specific binding of [^{3}H]-BTX-B by DNB-AB. DNB-AB shows irreversible inhibition of the binding of [^{3}H]-BTX-B (50 nM) to sheep brain synaptoneurosomes at 37°C. In the first bar, synaptoneurosomes incubated with 15 M DNB-AB for 30 min at 37°C, then exposed to hand held UV lamp at a distance of 5 cm (light intensity at source 0.46 W/cm^2) for 1 min, were then tested for [^{3}H]-BTX-B binding activity as described in Materials and Methods. After exposure to DNB-AB in the presence of UV light, subsequent binding of [^{3}H]-BTX-B was only 23 ± 4%, (mean ± SEM) of control binding. In the absence of UV light, the effect of 15 M DNB-AB was highly reversible and binding of [^{3}H]-BTX-B returned to 82 ± 5% (mean ± SEM) of control binding. Synaptosomes held at 37°C in the absence of DNB-AB, then exposed to UV light as described above showed altered [^{3}H]-BTX-B binding (70 ± 4% of control). Synaptosomes incubated with 500 M bupivacaine for 30 min, then exposed to UV light as described, washed, and assayed for [^{3}H]-BTX-B binding showed binding similar to synaptosomes exposed to UV light alone (70 ± 2% of control). Synaptosomes exposed to DNB-AB in the presence of UV light but protected with 500 M bupivacaine bound 51 ± 2% of control [3H]-BTX-B.

DISCUSSION

The results of this paper demonstrate light-dependent, irreversible inhibition of sodium current and [^{3}H]-BTX-B binding by the photoaffinity local anesthetic,

DNB-AB. This drug has relatively high affinity, for both aspects of inhibition have apparent IC_{50} values close to those for the traditional local anesthetic, bupivacaine (IC_{50} (I_{Na}) = 45 μM, Wang and Wang, 1992; IC_{50}(BTX) = 5.4 μM; McNeal et al., 1984).

Like many traditional LAs, DNB-AB has phasic blocking activities giving larger, faster developing inhibition during higher frequencies of depolarization. However, unlike most tertiary amine LAs, no resting (tonic) block was detectable with DNB-AB (at 20 μM) and the observed decrease in Na channel availability, previously characterized as an increase in apparent inactivation (Courtney, 1975; Hille, 1977), was not detectable with DNB-AB. Instead, an intrapulse decline in I_{Na} relative to control currents occurred with DNB-AB in the dark. Currents were reduced continuously during the period of depolarization when channels were open, but further block did not develop with the application of longer depolarizations, which would keep channels inactivated. These kinetics of inhibition are consistent with the selective binding of this LA to the open conformation of the channel, as has been seen with many compounds blocking K^+ channels (Armstrong, 1969; Armstrong and Hille, 1973; Castle, 1990) but with few LAs acting on normally gating Na^+ channels (Strichartz, 1973; Courtney, 1975; Hille, 1977; Neumcke, Schwarz, and Stampfli, 1981). Exceptionally, the drug quinidine, which has local anesthetic properties, has been shown to produce selective block of open channels (Colatsky, 1982; Hondeghem and Katzung, 1984).

Recovery of Na currents to the activatable state after phasic block was slowed by the drug, with both rapid and slow phases being effected. In particular, the fraction of current recovering with a 3–4 s time constant was about quadrupled with no real change in τ. In this respect, DNB-AB mimics the slow inactivating actions of some other local anesthetics (Khodorov, Shiskova, Peganov, and Revenko, 1976). In general, traditional local anesthetics such as lidocaine and bupivacaine interact with Na channels in the resting, open and inactivated states (Courtney, 1975; Hille, 1977; Schwarz, Palade, and Hille, 1977), and even in some pre-open states (Gillam, Starmer, and Grant, 1989; Chernoff, 1990). In this respect, DNB-AB appears to have uniquely selective properties as a local anesthetic and may provide more specific state-dependent binding than other LAs.

The irreversible, light-dependent inhibition by DNB-AB occurred in GH_3 cells during periods of minimal stimulation (5 min; 0.03 Hz). Occupancy of Na^+ channels by the drug under these conditions still produced a sizable (e.g., 40%) covalent binding, which was nearly completely prevented in the presence of high concentrations of bupivacaine. It thus appears that DNB-AB is near a blocking site where it can be covalently bound, even when the channels are not open, and from which it can be displaced by bupivacaine. Bupivacaine's actions may be due to spatial overlap (steric hindrance) with DNB-AB at a common binding site or to allosteric inhibition due, for example, to bupivacaine's binding to and stabilization of closed states of the channel that thus abolishes gating activation to the states with affinity for DNB-AB. The data here do not provide a way to discriminate between these possibilities.

Exposure of the drug to synaptosomal Na^+ channels in the light also reveals irreversible inhibition, protected by bupivacaine. Synaptosomes prepared by a similar technique have resting potentials of −40 to −60 mV (Creveling, McNeal, McCulloh,

and Daly, 1980). At this potential, few Na^+ channels open, yet many are still covalently labeled by DNB-AB. 77% of [^{3}H]-BTX-B binding could not be recovered suggesting that 77% of channels become permanently altered during the cross-linking experiment. Experiments under identical conditions with the addition of 500 μM bupivacaine irreversibly altered only 49% of channels. One interpretation of this result is that 77–49% or 28% of bound channels become cross-linked at a site which is coupled either sterically or allosterically to the bupivacaine site.

The dark equilibrium block of I_{Na} of 85% upon washout after UV illumination recovers to 42% of preexposure current. Therefore, 58% of DNB-AB bound channels fail to conduct after cross-linking. In control experiments using UV light, DNB-AB and 1 mM bupivacaine, 73% of blocked channels recovered function after washout. Therefore, only 27% of channels were rendered permanently nonfunctional. One interpretation is that ~30% of the loss of I_{Na} was protected by 1 mM bupivacaine and can be explained by cross-linking of DNB-AB at a site coupled sterically or allosterically to the bupivacaine binding site.

The irreversible inhibitions can not be explained by the action of UV light alone on the cells. In prior experiments (von Muralt and Stämpfli, 1953), UV light was shown to have a significant effect on sodium conductance in node of Ranvier, and on STX binding (Wiegele and Barchi, 1980). Other experiments have also shown that the effects of UV on Na^+ channel function are dependent on the membrane potential of the conducting tissue (Fox, 1974).

We found that UV light alone had little effect on I_{Na} when GH_3 cells were held at −100 mV. Therefore, the UV light activates DNB-AB to cause a permanent effect on I_{Na}, either by cross-linking the ligand at the site of physiologic activity or by transforming DNB-AB and disrupting Na^+ channel function.

In experiments on sheep brain synaptosomes, again the binding of DNB-AB in the absence of UV light can be shown to be highly reversible (82 ± 5%). However, when drug exposures are done in the presence of UV light, the binding of [^{3}H]-BTX-B is irreversibly inhibited (23 ± 4%). The effect of UV light on [^{3}H]-BTX-B binding in the absence of DNB-AB was significant (loss of 30 ± 4% of binding), however, it was still significantly less than the effect of UV light on [^{3}H]-BTX-B binding in the presence of 15 μM DNB-AB.

In conclusion, we have synthesized a local anesthetic, DNB-AB, which shows conventional albeit more state selective inhibition of Na channels. When exposed to UV light, DNB-AB irreversibly affects both I_{Na} and [^{3}H]-BTX binding, two assays associated with conventional LAs. Prior studies of model local anesthetics which form covalent cross-linking to the site of physiologic activity have used only inhibition at [^{3}H]-BTX-B binding as an assay at local anesthetic activity (Gusovsky, Nishizawa, Padgett, McNeal, Rice, Kim, and Creveling, 1990; Creveling, Bell, Burke, and Chang, 1990). This ligand, DNB-AB, with a relatively high affinity and an apparently strong state-dependent selectivity for Na^+ channels, should prove useful in biochemical studies of the LA binding site(s).

We thank Dr. John Maggio of Harvard Medical School for help with the NMR experiments and advice about the chemistry. Hal Feldman, D.Sc. generously dissected and donated the sheep brain. Dr. Jonathan Cohen, Harvard Medical School, provided thoughtful advice on the photo-protection

experiments. John McHugh is a medical student in the joint Harvard-MIT Program in Health Sciences and Technology.

The research was supported by NIH Grant (to G. R. Strichartz) GM15904 at the Harvard Anesthesia Center for Research and Training.

Original version received 9 May 1994 and accepted version received 23 September 1994.

REFERENCES

Aldrich, R. W., D. P. Corey, and C. F. Stevens. 1983. A reinterpretation of mammalian sodium channel gating based on single channel recording. *Nature.* 306:436–441.

Armstrong, C. M., and W. F. Gilly. 1992. Access resistance and space clamp problems associated with whole cell patch clamping. *Methods in Enzymology.* 207:100–122.

Armstrong, C. M. 1969. Inactivation of the potassium conductance and related phenomenon caused by quaternary ammonium ion injection into squid axons. *Journal of General Physiology.* 54:553–575.

Armstrong, C. M., and F. Benzanilla. 1974. Charge movement associated with the opening and closing of the activation gates of the Na channels. *Journal of General Physiology.* 63:533–552.

Bezanilla, F., and C. M. Armstrong. 1977. Inactivation of the sodium channel I. Sodium current experiments. *Journal of General Physiology.* 70:549–566.

Brown, G. B., S. C. Tieszen, J. W. Daly, J. E. Wernick, and E. X. Albequerque. 1981. Batrachatoxinin-A 20 α-benzoate: a new radioactive ligand for voltage-sensitive sodium channels. *Cellular and Molecular Neurobiology.* 1:19–40.

Butterworth, J. F., and G. R. Strichartz. 1990. Molecular mechanisms of local anesthesia: a review. *Anesthesiology.* 72:711–734.

Castle, N. A. 1991. Selective inhibition of potassium currents in rat ventricle by clofilium and its tertiary homolog. *The Journal of Pharmacology and Experimental Therapeutics.* 257:342–350.

Castle, N. A. 1990. Bupivacaine inhibits the transient outward K^+ but not the inward rectifier in rat ventricular myocytes. *Journal of Pharmacology and Experimental Therapeutics.* 255:1038–1046.

Catterall, W. C., C. S. Morrow, J. W. Daly, and G. B. Brown. 1981. Binding of Batrachotoxinin A 20-a-benzoate to a receptor site associated with sodium channels in synaptic nerve ending particles. *Journal of Biological Chemistry.* 256:8922–8927.

Chernoff, D. M., and G. S. Strichartz. 1990. Kinetics of local anesthetic inhibition of neuronal sodium currents. *Biophysical Journal.* 58:69–81.

Chernoff, D. M. 1990. Kinetic Analysis of phasic inhibition of neuronal sodium currents by lidocaine and bupivacaine. *Biophysical Journal.* 58:53–68.

Colatsky, T. J. 1982. Quinidine block of cardiac sodium channels is rate and voltage dependent. *Biophysical Journal.* 37:343*a*. (Abstr.)

Cota, G., and C. M. Armstrong. 1989. Sodium channel gating in clonal pituitary cells: the inactivation step is not voltage dependent. *Journal of General Physiology.* 94:213–232.

Courtney, K. R. 1975. Mechanism of frequency dependent inhibition of sodium currents in frog myelinated by the lidocaine derivative GEA-968. *Journal of Pharmacology and Experimental Therapeutics.* 195:225–236.

Courtney, K. R. 1980. Structure activity relations for frequency-dependent sodium channel block in nerve by local anesthetics. *Journal of Pharmacology and Experimental Therapeutics.* 213:114–119.

Creveling, C. R., M. E. Bell, T. R. Burke, E. Chang, G. A. Lewandowski-Louerburgh, K. Chang-Ho, K. C. Rice, and J. W. Daly. 1990. Procaine isothiocyanoate: an irreversible inhibitor of the specific binding of [^{3}H]batrachotoxinin-A benzoate to sodium channels. *Neurochemistry Research.* 15:441–448.

Creveling, C. R., E. T. McNeal, D. H. McCulloh, and J. W. Daly. 1980. Membrane potentials in cell-free preparations from guinea pig cerebral cortex: effect of depolarizing agents and cyclic nucleotides. *Journal of Neurochemistry.* 35:922–932.

Dodd, P. R., J. A. Hardy, A. E. Oakley, J. A. Edwardson, E. K. Perry, and J. P. Delaunoy. 1981. A rapid method for preparing synaptosomes: comparison with alternative methods. *Brain Research.* 226:107–118.

Fleet, G. W. J., J. R. Knowles, and R. R. Porter. 1972. Labeling of a specific antibody against the photo-precursor of an aryl nitrene. *Biochemical Journal.* 128:499–508.

Fox, J. M. 1974. Selective blocking of the nodal sodium channels by ultraviolet radiation II. The interaction of Ca^{+2}, H^+, and membrane potential. *Pflügers Archiv.* 351:303–314.

Gillam, F. R., III, C. F. Starmer, and A. O. Grant. 1989. Blockade of rabbit atrial sodium channels by lidocaine characterization of continuous end frequency dependent blocking. *Circulation Research.* 65:723–739.

Gusovsky, F., Y. Nishizawa, W. Padgett, E. T. McNeal, K. Rice, C. H. Kim, C. R. Creveling, and J. W. Daly. 1990. Voltage dependent sodium channels in synaptoneurosomes: studies with $^{22}Na+$ influx and [^{3}H]saxitoxin and [^{3}H] batrachotoxinin A 20-α-benzoate binding. Effects of proparacaine isothiocyanate. *Brain Research.* 518:101–106.

Hahin, R., and G. R. Strichartz. 1981. Effects of deuterium oxide on the rate and dissociation constants for saxitoxin and tetrodotoxin action. *Journal of General Physiology.* 78:113–139.

Hamill, O. P., A. Marty, E. Neher, B. Sackmann, and F. J. Sigworth. 1981. Improved patch clamp techniques for high resolution current recording from cells and cell-free membrane patches. *Pflügers Archiv.* 391:85–100.

Hanck, D. A., and M. F. Sheets. 1992. Time dependent changes in kinetics of Na^+ current in single canine lining cardiac Purkinje cells. *American Journal of Physiology.* 262:H1197–1207.

Hill, R. J., H. J. Duff, and R. S. Sheldon. 1988. Determinants of stereospecific binding of type I antiarrhythmic drugs to cardiac sodium channels. *Molecular Pharmacology.* 34:659–663.

Hille, B. 1977. Local anesthetics. Hydrophobic and hydrophilic pathways for the drug-receptor reaction. *Journal of General Physiology.* 69:497–515.

Hille, B. 1992. Ion Channels of Excitable Membranes. Second edition. Sinauer Associates, Inc. Sunderland, MA. 390–422.

Hille, B. 1980. Theories of anesthesia: general perturbations versus specific receptors. *In* Molecular Mechanisms of Anesthesia: Progress in Anesthesiology. Vol. 2 B. R. Fink, editor. Raven Press, New York. 1–5.

Hondeghem, L. M., and B. G. Katzung. 1977. Time and voltage-dependent interaction of Antiarrhythmic drugs with cardiac sodium channels. *Biochimica Biophysica Acta.* 472:373–398.

Hondeghem, L. M., and B. G. Katzung. 1984. Antiarrhythmic agents: the modulated receptor mechanism of action of sodium and calcium channel-blocking drugs. *Annual Review of Pharmacology and Toxicology.* 24:387–423.

Ji, T. H. 1979. The application of chemical crosslinking for studies on cell membranes and the identification of surface reporters. *Biochimica et Biophysica Acta.* 559:39–69.

Khodorov, B. L., L. Shishkova, F. Peganov, and S. Revenko. 1976. Inhibition of sodium currents in frog Ranvier node treated with local anesthetics: role of slow sodium inactivation. *Biochimica et Biophysica Acta.* 433:409–435.

LeeSon, S. L., G. K. Wang, A. Concus, E. Crill, and G. Strichartz. 1992. Stereoselective inhibition of neuronal sodium channels by local anesthetics: evidence for two sites of action? *Anesthesiology.* 77:324–335.

McNeal, E. T., G. A. Lewandowski, J. W. Daly, and C. R. Creveling. 1985. [^{3}H] Batrachotoxinin A 20-α-benzoate binding to voltage sensitive sodium channels: a rapid and quantitative assay for local anesthetic activity in a variety of drugs. *Journal of Medicinal Chemistry.* 28:381–388.

Neumcke, B., W. Schwarz, and R. Stampfli. 1981. Block of Na channels in the membrane of myelinated nerve by benzocaine. *Pflügers Archiv.* 390:230–236.

Peterson, G. L. 1977. A simplification of the protein assay method of Lowry et al. Which is generally more applicable. *Analytical Biochemistry.* 83:346–356.

Postma, S. W., and W. A. Catterall. 1984. Inhibition of binding of [^{3}H] batrachotoxinin A-20-α benzoate to sodium channels by local anesthetics. *Molecular Pharmacology.* 25:219–227.

Rando, T. A., G. K. Wang, and G. R. Strichartz. 1985. The interaction between the activator agents batrachotoxin and veratridine and the gating processes of neuronal sodium channels. *Molecular Pharmacology.* 29:467–477.

Schrock, A. K., and G. B. Schuster. 1984. Photochemistry of phenyl azide: chemical properties of the transient intermediates. *Journal of the American Chemical Society.* 106:5228–5234.

Schwarz, W., P. T. Palade, and B. Hille. 1977. Local anesthetics effect of pH on use-dependent block of sodium channels in frog muscle. *Biophysical Journal.* 20:343–368.

Sheldon, R. S., N. J. Cannon, and H. J. Duff. 1987. A receptor for type I anti-arrhythmic drugs associated with rat cardiac sodium channels. *Circulation Research.* 61:492–497.

Starmer, C. F., A. O. Grant, and H. S. Strauss. 1984. Mechanisms of use-dependent block of sodium channels in excitable membranes by local anesthetics. *Biophysical Journal.* 46:15–27.

Strichartz, G. R. 1973. The inhibition of sodium currents in myelinated nerve by quaternary derivatives of lidocaine. *Journal of General Physiology.* 62:37–47.

Strichartz, G. R. 1982. Structure of the saxitoxin binding site at sodium channels in nerve membranes. *Molecular Pharmacology.* 21:343–350.

Takmun, M. M., and W. A. Catterall. 1981. Ion flux studies of voltage sensitive sodium channels in synaptic nerve ending particles. *Molecular Pharmacology.* 19:78–86.

von Muralt, A., and R. Stämpfli. 1953. Dic Photochemische Wirkung von Ultraviolett licht auf ser erregten Ranvierischen Kroten der einzflenen nervenfuse. *Helvetica Physiologica Acta.* 11:182–193.

Wang, G. K., and S. Y. Wang. 1992. Altered stereoselectivity of cocaine and bupivacaine isomers in normal and Batrachotoxin modified Na channels. *Journal of General Physiology.* 100:1003–1020.

Wang, G. K., and G. R. Strichartz. 1983. Purification and characterization of neurotoxins from venoms of the scorpions centruroides sculptatus and *Leiurus quinquestriatus*. *Molecular Pharmacology.* 23:519–533.

Weigele, J. B., and R. L. Barchi. 1980. Ultraviolet irradiation produces loss of saxitoxin binding to sodium channels in rat synaptosomes. *Journal of Neurochemistry.* 35:430–435.

Willow, M., T. Gonoit, S. W. Postma, and W. A. Caterall. 1986. Inhibition of voltage-sensitive sodium channels by local anesthetic and anti-convulsants. *In* Molecular and Cellular Mechanisms of Anesthetics. S. H. Roth and K. W. Miller, editors. Plenum Publishing Corp., NY. 243–258.

Yeh, J. Z. 1980. Blockage of sodium channels by stereoisomers of local anesthetics. *In* Molecular Mechanisms of Anesthesia. Vol. 2. B. R. Fink, editor. Raven Press, New York. 35–44.